EFFECTIVE INTERACTIONS, MEDIUM MODIFICATIONS AND NEW NN–INTERACTIONS[1]

H.V. von Geramb, M. Sander and L. Jäde

Theoretische Kernphysik, Universität Hamburg
Luruper Chaussee 149, D–22761 Hamburg

Introduction

Optical model potentials (OMP) are the best available description for nucleon–nucleus (NA) scattering of low and medium energy projectiles with the only requirement to know the nucleus and its density distribution. The driving agent is supposed to be the nucleon–nucleon (NN) interaction. An appraisal of OMP ideas and developments can be found in the book by Feshbach [1]. The notion *effective interaction* is used to signal medium modifications of NN interactions, potentials and scattering amplitudes which enter in nonrelativistic and relativistic OMP calculations. Pauli blocking and mean field corrections are the predominant medium effects and they have consistently been used in effective interaction calculations [2]. We show in Fig. 1 a result calculated with the Hamburg effective interaction of 1982. Newly established are corrections which modify directly meson and nuclear properties of boson exchange models [3].

Effective interactions are used in different contexts and a restriction of the notion, as it is used here, appears necessary. We associate with an effective interaction an operator which contains only variables and reference parameters which can be specified *a posteriori* for any nuclear target. This approach fuses an NN interaction with a many body scattering theory *a priori* and, after target specification, a modest calculation yields readily the OMP. Developments of t–matrices and nuclear matter g–matrices have always supported this line of thought and *folding models* comprise methods and algorithm for the fusion of effective interactions (including the phenomenological effective interactions) with a specific nucleus. We are here only concerned about some features of effective interactions.

Watson multiple scattering theory and KMT use the two body t–matrix which can be derived i.) from the experimental free t–matrix [4], ii.) two body t–matrices computed from some meson exchange model, of which Nijmegen, Paris [5] and Bonn [6] are representative and our nonlinear meson exchange model is in progress [7], iv.) phenomenological NN potentials — Hamada–Johnston, Reid and some of Nijmegen [8] and v.) quantum inversion potentials determined directly from NN partial wave phase shifts [9]. The nuclear matter approach of the OMP uses Brueckner theory and the two body g–matrix, in connection with local density approximation (LDA), as effective interaction [10]. The g–matrix can be calculated from any of the mentioned NN potentials. Relativistic effective interactions have also been proposed but have never reached the popularity as nonrelativistic formulations. The relativistic Dirac OMP, initiated by Walecka and made a success by Clark et al. [2], belongs to another class and does not use the concept of an effective NN interaction.

Several potential models give on–shell equivalent best fits to the newest NN data but are off–shell not equivalent due to differing nonlocalities. The dispute about the importance of nonlocality has also hit effective interaction and OMP calculations. Few–body calculations show surprisingly little to now difference due to off–shell differences with the exception of nuclear matter saturation and equilibrium or the triton binding energy [11]. Phenomenological three body forces can heal the problem but the results are not generally accepted. An inclusion of three body forces in OMPs have not been seriously considered. We shall be concerned about the off–shell differences in effective interactions and their effects upon the OMP and elastic scattering observables respectively. These results have been numerically realized by Dr. Arellano during a recent visit in Hamburg and we shall concentrate on some relevant results and conclusions from this work [12]. Finally, some preliminary studies for the σ–meson, as a candidate for mesonic medium modifications, is given.

[1]Specialists' Meeting on the Nucleon–Nucleus Optical Model up to 200 MeV, Commissariat à l'Energie Atomique, Bruyères-le-Châtel (France), 13.–15. November 1996, Organised by the OECD Nuclear Energy Agency Nuclear Science Committee and the Commissariat à l'Energie Atomique, Bruyères-le-Châtel

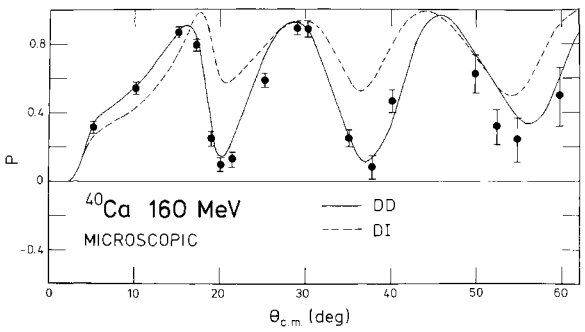

Figure 1: ^{40}Ca(p,p) at 160 MeV. This classical result is supposed to demonstrate the importance of medium effects.

Effective Interactions

The nuclear matter approach uses the two body t– and g–matrix as effective interaction. The standard approach is a q–space representation of the Lippmann–Schwinger equation in partial waves

$$t_{\ell\ell'}(p,p';E(k)) = V_{\ell,\ell'}(p,p') - \frac{2}{\pi}\int_0^\infty \sum_j V_{\ell j}(p,q)\frac{1}{q^2-k^2-i\eta}t_{j\ell'}(q,p';k)q^2dq, \tag{1}$$

and similarly the Brueckner–Bethe–Goldstone equation for nuclear matter

$$g_{\ell\ell'}(p,p';k_F,E(k)) = V_{\ell,\ell'}(p,p') - \tag{2}$$
$$\frac{2}{\pi}\int_0^\infty \sum_j V_{\ell j}(p,q)\frac{\mathcal{Q}(q,K;k_F)}{e(q,K;k_F)-e(k,K;k_F)-i\eta}g_{j\ell'}(q,p';k_F,E(k))q^2dq$$

with angle averaged Pauli blocking $\mathcal{Q}(q,K;k_F)$ and a single particle energy

$$e(q,K;k_F) = \frac{\hbar^2}{m}(q^2+K^2) + \mathcal{U}(q,K;k_F,\alpha). \tag{3}$$

which contains the crucial self energy $\mathcal{U}(q,K;k_F)$. To be more specific, we often use the Paris potential in momentum space, but traditionally as a momentum dependent interaction in r–space

$$V(r,p^2) = V_a(r) + \frac{p^2}{m}V_b(r) + V_b(r)\frac{p^2}{m} \quad \text{with} \quad p^2 = -\hbar^2\left(\frac{1}{r}\frac{d^2}{dr^2}r - \frac{L^2}{r^2}\right). \tag{4}$$

For the evaluation of half off–shell t–matrices we are using the Van Leeuwen and Reiner [13] extension of off–shell wave functions by the inhomogeneous Schrödinger equation

$$\left[k^2 + \frac{\mathrm{d}^2}{\mathrm{d}r^2} - \frac{\ell(\ell+1)}{r^2} - V_\ell(r)\right]\,\psi_\ell(k,q,r) = (k^2-q^2)\,u_\ell(qr). \tag{5}$$

$$\left[k^2 + (1+2V_b(r))\left(\frac{\mathrm{d}^2}{\mathrm{d}r^2} - \frac{\ell(\ell+1)}{r^2}\right) - V^a(r)\right.$$
$$\left. + V_b''(r) + 2V_b'(r)\frac{\mathrm{d}}{\mathrm{d}r}\right]\psi_\ell(k,q,r) = (k^2-q^2)\,u_\ell(qr).$$

The solution $\psi_\ell(k,q,r)$ vanishes at the origin and its asympotic behavior is

$$\lim_{r\to\infty}\psi_\ell(k,q,r) = u_\ell(qr) - q\,w_\ell^{(+)}(kr)\,T_\ell(k,q;k^2). \tag{6}$$

For coupled systems this procedure requires

$$\left[-\frac{d^2}{dr^2}+\frac{\ell(\ell+1)}{r^2}-k^2\right]\psi^{JST}_{\ell',\ell}(k,q,r)+\sum_{\ell''}V^{JST}_{\ell',\ell''}(r)\psi^{JST}_{\ell'',\ell}(k,q,r)=(k^2-q^2)\delta_{\ell',\ell}u_\ell(qr), \tag{7}$$

and

$$\lim_{r\to\infty}\psi^{JST}_{\ell',\ell}(k,q,r)=\delta_{\ell',\ell}u_\ell(qr)-qw^+_\ell(kr)T^{JST}_{\ell',\ell}(k,q;k^2). \tag{8}$$

Coulomb corrections can be readily included but, generally, a Coulomb interaction is added to the hadronic OMP using a homogeneous charged sphere or Fermi distribution. From the half off–shell wave function the fully off–shell t–matrix can be computed but we shall not make use of it in this contribution. Inverse scattering theory was used to determine local, energy independent r–space NN potentials with the purpose to compare them as on–shell equivalent to the genuine Paris and Bonn–R momentum dependent potentials [14].

Some well known expressions are used for discussions. The half off–shell t-matrix

$$t_\ell(p,k;E)=-\frac{1}{p}\left(\frac{m}{\hbar^2}\right)\int_0^\infty j_\ell(pr)V_\ell\psi_\ell(k,r)dr$$

$$t_\ell(p,k;E)=\left(\frac{p}{k}\right)^\ell t_\ell(k,k;E)+\frac{p^2-k^2}{p}\int_0^\infty j_\ell(pr)\zeta_\ell(k,r)dr$$

with the healing function

$$\zeta_\ell(k,r)=\psi_\ell(k,r)-j_\ell(kr)-t_\ell(k,k;E)h^+_\ell(kr)=z_\ell(k,r)e^{i\delta_\ell(k)}.$$

A convenient measure of the half off–shell continuation is the Kowalski–Noyes f–ratio

$$f_\ell(p,k;e)=\frac{t_\ell(p,k;e)}{t_\ell(k,k;e)}.$$

In-Medium Full–Folding Optical Potential

The OMP is formulated as an antisymmetrized convolution of an effective interaction with the target ground state. The target is described within a shell model which is fitted to reproduce elastic electron scattering charge form factors and other structure relevant properties. For nuclei off the stability line or in an excited state one relies on theoretical predictions. The nuclear matter approach identifies the reaction matrix as *effective interaction* with the implication that this reduces at higher energies to the t–matrix. The results and conclusions of a most complete calculation is reproduced next [12].

A calculable expression for the optical potential *in medium* emerges after a systematic reduction of the many body propagator when represented in terms of the target ground state spectral function [15]. To lowest order in a series expansion of the two-body propagator in a finite nucleus, this interaction can be identified with the g–matrix solution of the Brueckner-Bethe-Goldstone equation for interacting nucleons in infinite nuclear matter and evaluated at nuclear density $\rho(R)$ in the nucleus. This interaction retains nuclear medium correlations associated with the nuclear mean fields and Pauli blocking. The *in-medium* full–folding optical potential then reads

$$\begin{aligned}U(\vec{k}\,',\vec{k};E) &= \frac{4}{(2\pi)^3}\int d\vec{R}\,e^{i\vec{q}\cdot\vec{R}}\rho(R)\frac{1}{\hat{\rho}(R)}\int d\vec{P}\\ &\times\ \Theta[\hat{k}(R)-P]\left\langle\tfrac{1}{2}(\vec{K}-\vec{P}-\vec{q})\left|g_{\vec{K}+\vec{P}}(E+\overline{\epsilon}\,;\vec{R})\right|\tfrac{1}{2}(\vec{K}-\vec{P}+\vec{q})\right\rangle_A,\end{aligned} \tag{9}$$

with the definitions

$$\vec{K}=\tfrac{1}{2}(\vec{k}+\vec{k}\,')\,;\quad \vec{q}=\vec{k}-\vec{k}\,'\,. \tag{10}$$

Thus, the optical potential requires the calculation of g–matrices off–shell as their relative momenta obey no constraints apart from those imposed by the ground state mixed density of the target. Furthermore, no assumptions are introduced on the nature of the momentum dependence of the optical potential, thus retaining all non localities arising from the genuine momentum dependence of the NN effective interaction. Actual calculations involve determining g–matrices at several densities and over a wide range of total CM momenta, features fully accounted for in [12]. In Fig. 2 we show some off–shell t– and g–matrices for several potentials.

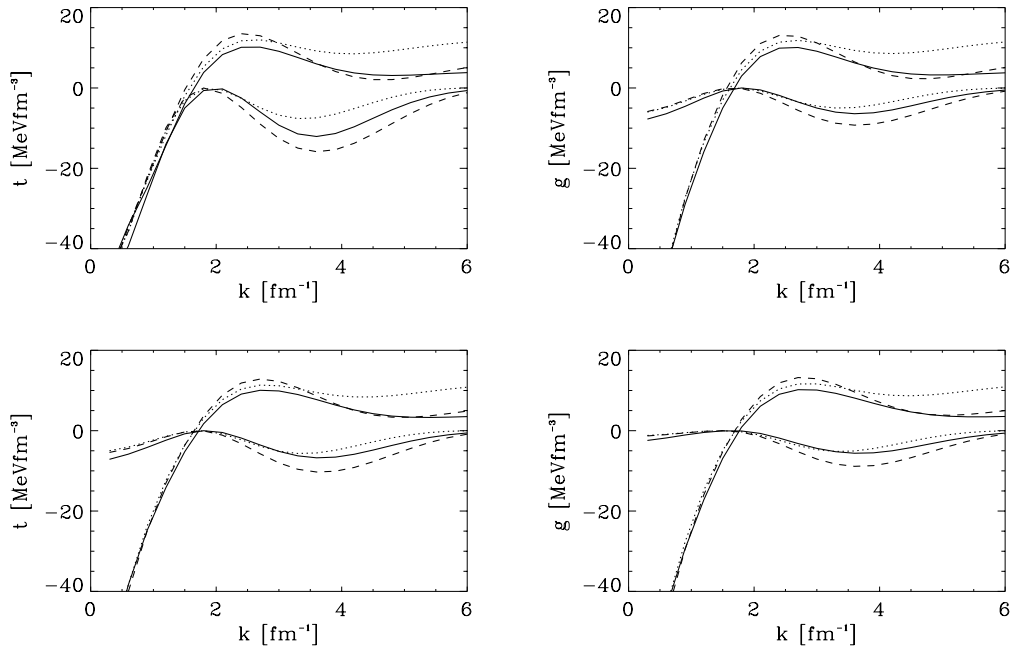

Figure 2: ${}^1S_0$ diagonal t– (left) and g– (right) matrices at $\omega = 30$ MeV (top) and $\omega = 200$ MeV (bottom). We show results for the SM94 inversion potential (full line), the original Paris potential (dotted) and the Par1.3 inversion potential (dashed).

In the context of a medium independent internucleon interaction, as when the free t–matrix is used to represent the NN effective interaction, the integral over the spatial coordinate can be performed separately from the motion of the target nucleons. Using the mixed density one recovers the expression for the full–folding optical potential in the zero density approximation [16], namely $U(\vec{k}\,', \vec{k}; E) \rightarrow U_o(\vec{k}\,', \vec{k}; E)$, where

$$U_o(\vec{k}\,', \vec{k}; E) = \int d\vec{P}\ \rho(\vec{P} + \tfrac{1}{2}\vec{q}, \vec{P} - \tfrac{1}{2}\vec{q}) \left\langle \tfrac{1}{2}(\vec{K} - \vec{P} - \vec{q}) \left| t_{\vec{K}+\vec{P}}(E + \overline{\epsilon}) \right| \tfrac{1}{2}(\vec{K} - \vec{P} + \vec{q}) \right\rangle_A \ . \tag{11}$$

The dependence of the optical potential on off–shell t–matrices becomes explicit in the above expression. The feasibility of the full–folding model to investigate particular signatures of the effective interaction off–shell will depend on the sensitivity of NA scattering observables to the use of t–matrices with manifestly distinctive behaviors off–shell. An important constraint for such study is that the effective interactions, t–matrices in this limit, agree on–shell. To the extent this constraint is met one can attain the differences in the NA scattering observables to the differences of the interactions off–shell.

A simple kinematical effect usually overlooked, but explicitly accounted for in these calculations, is that the full–folding approach calls for matrix elements of energy $E + \overline{\epsilon}$ in the laboratory frame. In the limit of the free t–matrix for the NN interactions, the energy of the interacting pair in its CM is given by $E + \overline{\epsilon} - \frac{1}{4m}(\vec{K} + \vec{P})^2$. Therefore, the maximum energy of the pair in its CM is $E + \overline{\epsilon}$, the energy of the beam plus the average binding energy of the target nucleons. In the case of optical potentials for nucleons at 500 MeV, for instance, t–matrices of up to $\sim$1 GeV in the laboratory frame are required. This more demanding sampling of the NN effective interaction is a result of the unconstrained kinematics allowed by the Fermi motion of the nucleons in the nucleus.

A few comments are pertinent regarding further approximations in the treatment of the t–matrix and which limit an assessment of the off–shell behavior of the NN interaction in NA scattering. A simplifying assumption, commonly used in alternative full–folding calculations [17, 18], is that the t–matrix varies very weakly with respect to the NN CM momentum $\vec{K} + \vec{P}$. Thus, the magnitude of this momentum is fixed to the (asymptotic) on–shell value of the incoming projectile, K_o, and the t–matrix is approximated by

$$t_{\vec{K}+\vec{P}}(\omega) \approx t_{\vec{K}_o}(\omega) \ . \tag{12}$$

Thus, t–matrices are evaluated at a fixed energy equal, in the NN CM, to one–half the energy of the beam. Here one has neglected all effects associated with the Fermi motion in the NN CM momentum dependence. The

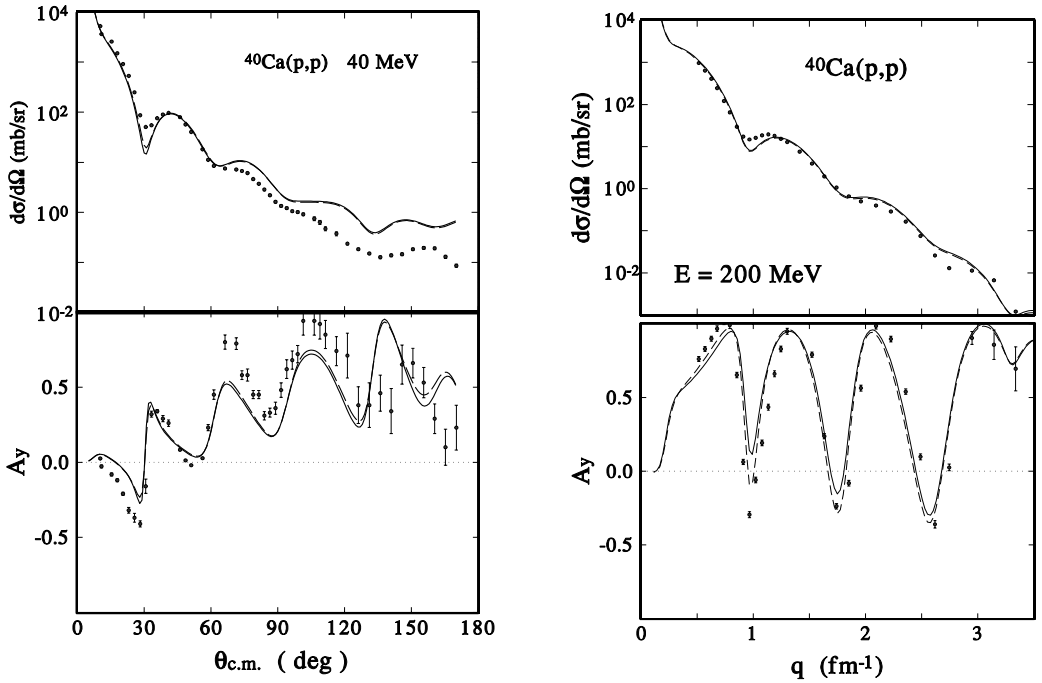

Figure 3: ^{40}Ca(p,p) at 40 MeV (left) and 200 MeV (right), taken from [12]. The genuine Paris Potential (dashed line), Paris inversion potential (solid line). In the cross section the two results are hardly to distinguish.

resulting full–folding calculations sample the t–matrix off–shell through the dependence on $\vec{P}$ in the relative momenta exclusively. This approximation seems adequate at beam energies near 300 MeV. Its application at lower or higher energies, however, needs further considerations as the NN t–matrix exhibits a sizable NN CM momentum dependence [19]. In the low energy region, apart from the fact that medium effects need to be incorporated in the model, the underlying kinematics prescribed by the full–folding leads to the sampling of the t–matrix in regions where it varies significantly as the low energy behavior of the interactions becomes dominant. In the high energy regime, in turn, difficulties arise from the opening of inelastic channels such as those associated with pion production or $\Delta-$resonances. The actual merit of the theory of the optical potential needs to be assessed with a consistent incorporation of such additional degrees of freedom.

Calculations of differential cross sections and analysing powers were made for proton elastic scattering for ^{40}Ca for 40 to 500 MeV. In Fig. 3 we compare results of the genuine Paris potential (dashed line) to a calculation using the phase equivalent inversion potential (full line). Using the inversion potentials based on SM94 does not alter this result. This confirms the high quality of the Paris potential at low energies. For both energies the differences are surprisingly small, which leads to the conclusion that OMPs are insensitive to given off–shell differences. The difference between theory and experiment at 40 MeV is not understood. In Fig. 4 we compare the calculation using the Paris potential with the results using the SM94 inversion potential (full line). At higher energies these calculations show that the use of the best available on-shell potentials is mandatory for the optical model.

Parametrization Scheme for Effective Interactions

We are making here reference to an algorithm which has been developed for the representation of t– and g–matrix elements [20] for its use in the program DWBA91 by J. Raynal [21]. This program is a completely restructured form of the well known antisymmetrized DWBA program by Schaefer and Raynal [22] and it includes now a fully consistent treatment of the elastic channel OMP and the transition operator using the same density dependent effective interaction. The OMP in r–space is fully antisymmetrized and the nonlocal OMP is numerically solved as integro–differential equation.

The input of DWBA91 requires the effective interaction to be a local operator in relative coordinates whose plane wave matrix elements optimally reproduce on– and off–shell g–matrix elements. As linear combination of operators we distinguish central, tensor, spin–orbit, quadratic spin–orbit and ℓ^2 terms. This decomposition

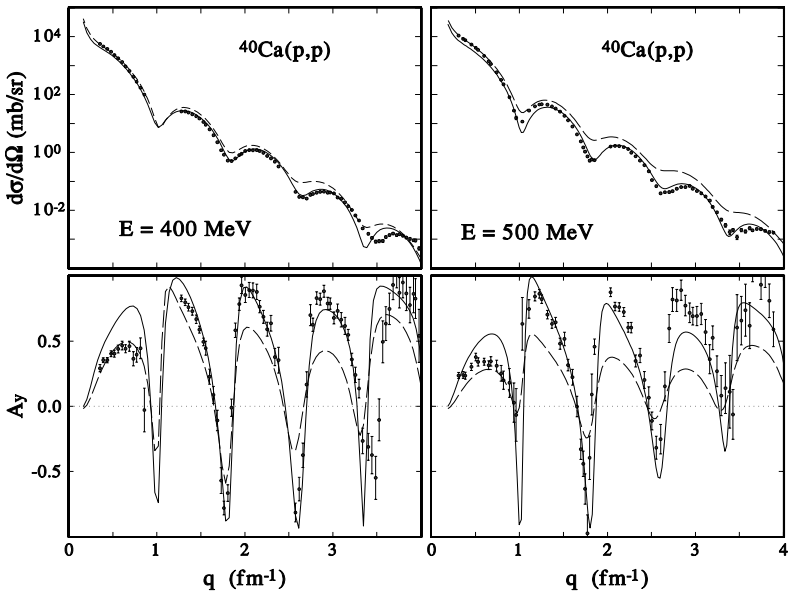

Figure 4: ^{40}Ca(p,p) at 400 MeV (left) and 500 MeV (right), taken from [12]. Paris inversion potential (dashed line), SM94 inversion potential (solid line).

is an extension of the traditional form used in inelastic NA scattering. The problem of interest is to match on– and off–shell matrix elements in accordance with DWBA91 input requirements

$$g_\alpha^{\rm eff}(q,k;E(k)) := \sum_{\beta=1}^{5}\sum_{i=1}^{n(\mu)} \langle q\alpha|\mathcal{O}_\beta(\mu_i)|k\alpha\rangle V_{\beta,i}(E), \quad \alpha = (L'LJST) \tag{13}$$

with

$$\mathcal{O}_\beta(\mu_i) = \left\{P_S, \vec{L}\cdot\vec{S}, S_{12}, L^2, (\vec{L}\cdot\vec{S})^2\right\} \frac{e^{-\mu_i r}}{r} P_T. \tag{14}$$

Ranges and strengths are χ^2 fitted using all partial waves $J \leq 4$ and using several hundred points of a discrete q,k mesh.

$$\begin{aligned} \vec{g}^{\ \rm eff}(\mu, V(E); q,k; E(k)) - \vec{g}(q,k;E(k))\omega_\alpha(q,k), \\ \vec{g} := (g_{\alpha_1}(q_1,k_1),\ldots,g_{\alpha_l}(q_m,k_n)) \end{aligned} \tag{15}$$

We are using SVD methods for minimizing the Euclidian norm with respect to strengths $V_{\beta,i}(E)$. Ranges μ_i were fixed *a priori* in the search. Results of this parametrization have been successfully used in $(pp\gamma)$ and $(np\gamma)$ Bremsstrahlung calculations [23].

NN–Potentials from Inverse Scattering and Boson–Exchange

Contrary to a derivation of NN potentials from a dynamical model, quantum inversion translates experimental phase shifts directly into a potential with the assumption of a radial Schrödiger equation as equation of motion for each partial wave. We have developed such inversion algorithm for single and coupled channel NN systems as well as for meson–nucleon and meson–meson scattering potentials [24, 9]. Inversion potentials reproduce, by dint of its construction, the input phase shifts with a local energy independent (but channel dependent) r-space potential. Such potentials have the advantage of extreme simplicity as compared with the meson exchange potentials which are generally nonlocal in q– as well as in r–space. It has been the goal of several recent investigations to find deficiencies of inversion potentials in comparison with meson exchange potentials with the purpose to find unique substructure effects. OMP calculations are one of the corner stones in this endeavour to see differences in microscopic optical model potentials which use either the meson theoretical Paris potentials with its explicit momentum dependence or the inversion potentials to the Paris potential phase shifts. Inversion guarantees only an exact on–shell equivalence of the two body t–matrix, but not of the g–matrix.

As fundamental equation of motion enters the radial Schrödinger equation for the two particle system

$$\left(-\frac{d^2}{dr^2}+\frac{\ell(\ell+1)}{r^2}+\frac{2\mu(E)}{\hbar^2}V_\ell(r)\right)\phi_\ell(r,k)=k^2\phi(r,k), \tag{16}$$

with the local potential $V_\ell(r)$ determined from the asymptotic phase shifts

$$\lim_{r\to\infty}\phi(r,k)=\exp(i\delta_\ell(k))\sin(kr-\frac{\ell\pi}{2}+\delta_\ell(k)). \tag{17}$$

This problem is solved with the Gelfand–Levitan–Marchenko integral equations for single and coupled channels. The results are the same for Gelfand–Levitan and Marchenko equations but the numerical part contains different hurdles. The Marchenko approach is given in its salient features.

In the Marchenko inversion enter the experimental data as S–matrix

$$S_\ell(k)=\exp 2i\delta_\ell(k) \tag{18}$$

for each partial wave. An input kernel is evaluated from this data

$$F_\ell(r,t):=-\frac{1}{2\pi}\int_{-\infty}^{\infty}h_\ell^+(rk)[S_\ell(k)-1]h_\ell^+(tk)\,dk. \tag{19}$$

The Marchenko fundamental equation

$$A_\ell(r,t)+F_\ell(r,t)+\int_r^\infty K(r,s)F(s,t)\,ds=0 \tag{20}$$

yields with the solution kernel $A_\ell(r,t)$ the potential

$$V_\ell(r)=-2\frac{d}{dr}A_\ell(r,r). \tag{21}$$

This algorithm applies in matrix form to coupled system of equations. The Gelfand–Levitan fundamental equations are using different boundary conditions and thus an input kernel which is calculated from the Jost–functions. The algorithm applies for all systems which can be cast into the form of a Sturm–Liouville equation which happily coincides directly with the radial Schroedinger equation.

We have calculated inversion potentials for many available phase shifts. The most reliable phase shift analyses are done at VPI by Arndt et al. [25] with a semiannual update and from Nijmegen whose results are used as PWA93 [8]. In Fig. 5 are given the inversion potential results from VZ40 (likely) the best available phase shift analysis below pion threshold. Other results, shown in the oral presentation, from PWA93 and FA96 can be obtained from the server [26] by anonymous ftp. The potentials reproduce the input phase shifts with a numerical error ≤ 0.02 degrees. It is obvious that the inversion approach implies the possibility to continue the on–shell t–matrix into the off–shell domain by inserting the inversion potentials into the Lippmann–Schwinger equation or Brueckner–Bethe–Goldstone equation. This is the most important result of inversion in contexts of OMP. Differences of off–shell continuations were shown in Fig. 2. In a comparison of our investigation of on–shell equivalent potentials we summarized the results in Figs. 3 and 4 and came to the conclusion that off–shell differences cannot be discerned from elastic NA scattering cross sections and spin observables. The need of NN potentials, which reproduce precisely the on–shell data, is necessary. An example to the later claim is given in Fig. 4. For energies below 200 MeV we confirm equivalence between the Paris, Bonn–B and inversion potentials from PWA93, SM95, VZ40 and VV40.

The quest for off–shell effects was reason enough to continue investigations with boson–exchange models. Some results of this solitary boson exchange model (OSBEP) are now available [7] and comparison with NN data are very encouraging. The purpose is to show that the description of NN data provided by OSBEP is comparable to Bonn–B, which is analogous in construction. As an important difference between OSBEP and Bonn–B, the empirical form factors used in the Bonn potential are not needed in OSBEP. This is achieved by applying a nonlinear dynamical model for the meson fields which tries to parameterize possible effects from QCD. In this context, an empirical scaling law is found to relate all meson parameters to the pion mass and self–interaction coupling constant. Thus, OSBEP is free of phenomenological form factors and the scaling law reduces the number of parameters with respect to the Bonn potential without deficiencies in the description of data.

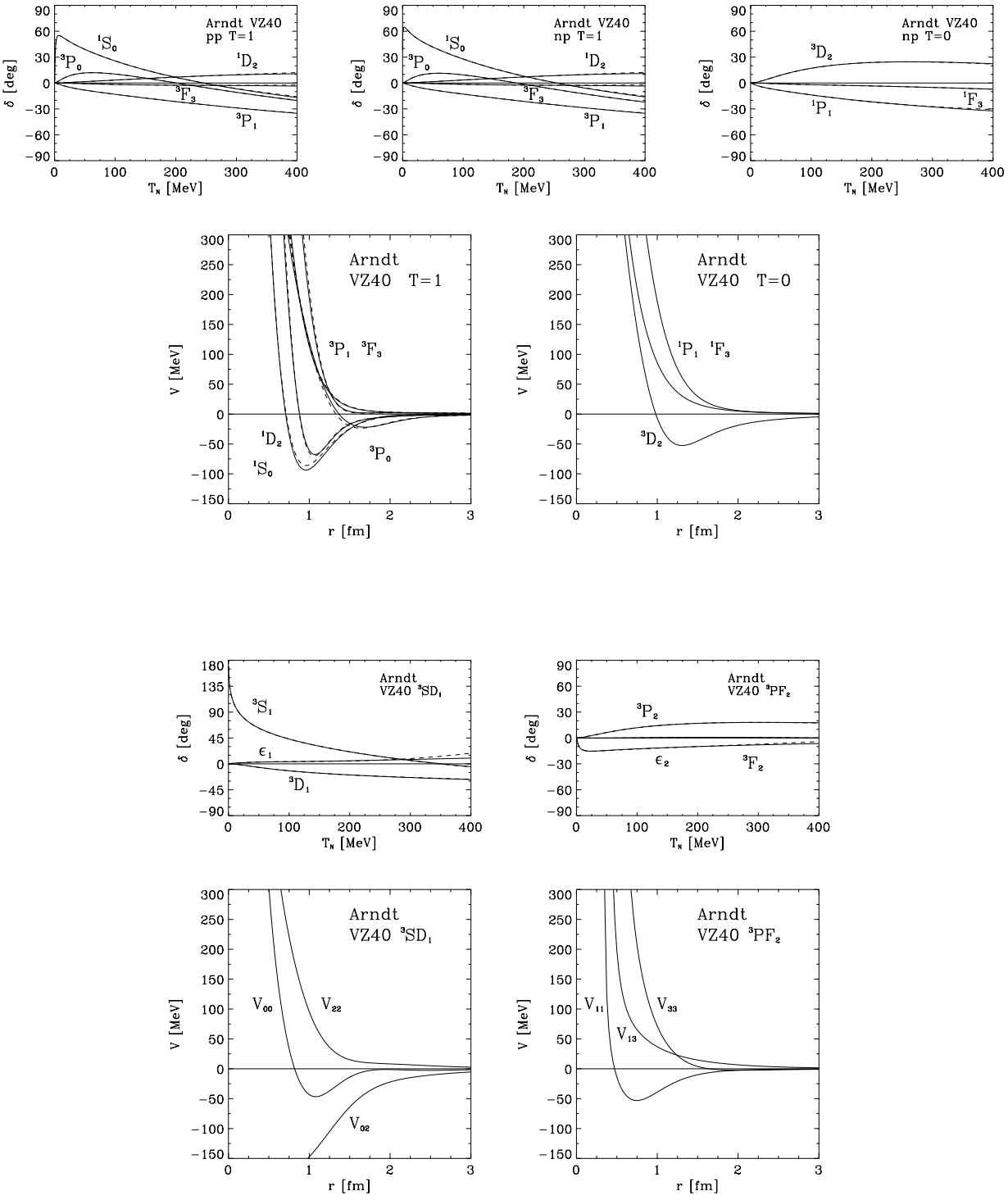

Figure 5: Arndt VZ40 phase shifts and inversion potentials.

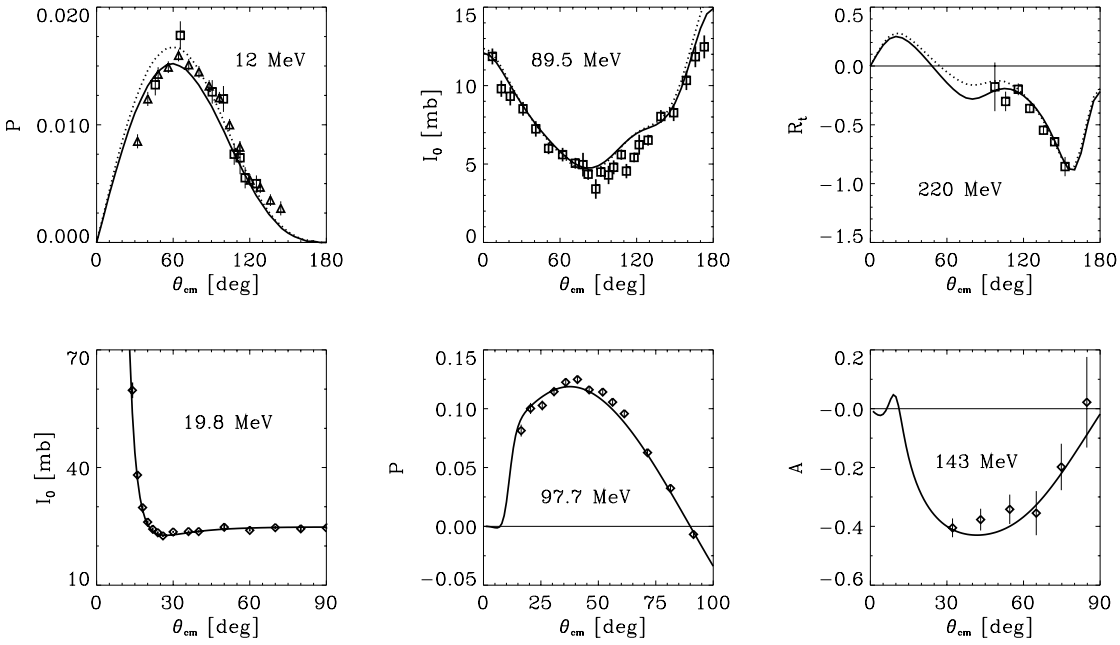

Figure 6: Observables of *np* scattering (top) and *pp* scattering (bottom) from OSBEP. Kinetic laboratory energy is denoted, experimental data taken from [25]. We show theoretical predictions from OSBEP (full) and Bonn–B (dotted).

Motivated by chiral invariant meson–baryon Lagrangians and spontaneous symmetry breaking, we use a Lagrangian

$$\mathcal{L}_\Phi = \frac{1}{2}\left(\partial_\mu\partial^\mu\Phi^2 - m^2\Phi^2\right) - \frac{\lambda_1}{2p+2}\Phi^{2p+2} - \frac{\lambda_2}{4p+2}\Phi^{4p+2} + \mathcal{L}_{int}, \tag{22}$$

in which Φ stands for the meson fields and $\mathcal{L}_{int}$ accounts for the interaction with nucleons and other fields. The nonlinearity is of utmost importance. The decoupled single meson fields satisfy a nonlinear Klein–Gordon equation (KGE)

$$\partial_\mu\partial^\mu\Phi + m^2\Phi + \lambda_1\Phi^{2p+1}\lambda_2\Phi^{4p+1} = 0. \tag{23}$$

This equation can be solved analytically by using the ansatz $\Phi = \Phi(\varphi)$, where φ is a wave solution of the linear KGE

$$\varphi(x,k) = \frac{1}{\sqrt{2\omega_k V D_k}}\, a(k)\, e^{-ikx} \quad \text{and} \quad \varphi^\dagger(x,k) = \frac{1}{\sqrt{2\omega_k V D_k}}\, a^\dagger(k)\, e^{ikx}, \tag{24}$$

where V is the volume of the system and D_k is a momentum dependent Lorentz–invariant function which is later used to guarantee finite self–scattering amplitudes. This substitution reduces (23) to an ordinary nonlinear differential equation which permits direct integration. The solutions are expressed as a power series in terms of φ and Gegenbauer polynomials

$$\Phi(\varphi) = \sum_{n=0}^{\infty} C_n^{1/2p}(w)\, b^n\, \varphi^{2pn+1}, \tag{25}$$

with

$$b = \left\{\left[\frac{\lambda_1}{4(p+1)m^2}\right]^2 - \frac{\lambda_2}{4(2p+1)m^2}\right\}^{\frac{1}{2}} \qquad \text{and} \qquad w = \frac{1}{b}\frac{\lambda_1}{4(p+1)m^2}.$$

These particular solutions $\Phi(\varphi)$ are *solitary meson fields*. In contrast to conventional models, the OSBEP uses the solitary meson states (25) instead of asymptotic free in– and out–states to define the propagator function. This yields the *solitary meson propagator* which in momentum space has the form

$$iP(k^2,m) = \sum_n \left[C_n^{\frac{1}{2p}}(w)\right]^2 (m^p\alpha)^{2n} \frac{(2pn+1)^{2pn-2}}{D_k^{2pn+1}\left(\vec{k}^{\,2} + M_n^2\right)^{pn}}\, i\Delta_F(k,M_n), \tag{26}$$

where $\alpha = b/(2mV)^p$, $M_n = (2pn+1)m$ and $i\Delta_F(k^2,m)$ denotes the Feynman propagator. The normalization D_k now is fixed to guarantee finite self–energy diagrams. It turns out, that this is also sufficient to regularize the NN scattering equation and thus no form factor is needed when the solitary meson propagator is used instead of the conventional Feynman propagator in a boson exchange potential. Additionally, the self–interaction coupling constants α_β ($\beta = \pi,\ \eta,\ \rho,\ \omega,\ \sigma_0,\ \sigma_1,\ \delta$) of the various mesons used in the boson exchange model obey the scaling relation

$$\alpha_\beta(m_\beta) = \sqrt{\kappa} \cdot \alpha_\pi \left(\frac{m_\pi}{m_\beta}\right)^p , \tag{27}$$

where $\kappa = 1$ for pseudoscalar and scalar mesons and $\kappa = 2$ for vector mesons. Therefore, the pion self–interaction coupling constant α_π is the only parameter to describe the meson dynamics. Together with the meson–nucleon coupling constants, the OSBEP thus contains a total number of nine parameters. The πNN coupling constant is set to the value $g_{\pi NN}/4\pi = 13.7$ suggested by Arndt [4], the remaining parameters are adjusted to fit NN phase shifts and deuteron properties. Finally, observables of *np* as well as *pp* scattering are obtained which agree very well with experimental data. The description of NN data by the OSBEP seems to be indeed comparable to the Bonn–B potential, see Fig. 6.

This model uses all mesons with a mass below 1 GeV and this includes the σ–meson with a mass ~ 500 MeV. We see in the σ–meson the best candidate for a fragile object which can easily be altered in its properties by external fields and generate an effective pion mass. Ultimately, it is intended to include the correlated two pion exchange with full dynamics in OSBEP but this seems still far from realization. Some auxiliary studies with inversion methods, applied to elastic $\pi\pi$ scattering in the L=0 and T=0 and 2 channels, are discussed next.

The $\pi\pi$ System and σ–Meson

Medium effects from meson and boson exchange models are related to restoration mechanisms of the broken ciral symmetry in nuclear matter. This effect is less well established than medium modifications due to Pauli blocking and mean fields. This field of research is presently in the center of different theoretical lines of thought and some of them are found in [3].

It is beyond any doubt that the correlated two pion exchange mechanism is important for the attractive medium range NN potential. We use our inversion algorithms [24] and generate an inversion potential for πN P_{33} scattering with the purpose to generate a potential which supports the $\Delta(1232)$–resonance. The result is shown in Fig. 7 (top) with the reproduced phase shifts and the hadronic interaction. Aspects of these potentials have been discussed at the Balaton conference [24]. One should draw the attention upon the short range potential barrier. A calculation for the $\pi\pi$, S=0, T=0 and 2 channels yields results shown in Fig. 7 (bottom). V_0^2 is a repulsive potential without any resonance support. The V_0^0 potential has a short range barrier which can support a resonance in the attractive pocket. It has been claimed that this is a resonance with a width of ~ 500 MeV. The δ_0^0 phase shift in this channel changes very smoothly, not like what is expected from a resonance, compare the ΦP_{33} resonance in Fig. 7. Meson exchange models are very specific about the $\sigma_0 \sim 500$ MeV mass. We investigated the phase shifts with respect to small changes of the pion mass. In Fig. 8 (left) results are shown for the δ_0^2 and δ_0^0 phase changes. The mass changes are typically 2.5% progressing from a–d, where b represents a calculation using the correct π^+ mass. These small changes simulate medium modifications of the pion mass. The changes do not affect the δ_0^2 phase but alter δ_0^0 drastically. This latter result was not expected. In another calculation we fix the total energy, $M_{\pi\pi} = 500$ MeV and vary the pion mass between 130–150 MeV ($2\mu = m_\pi$). The results are shown in Fig. 8 (right) for the δ_0^0 phase variation. It implies a resonance feature due to an effective mass of $m_\pi \pm 2$ MeV. This high sensitivity of the two–pion system may be an important medium effect which requires a more detailed study. We are concentrating our efforts upon this mechanism within the nonlinear boson exchange model but there exist several other theoretical approaches and experiments helping to ascertain the proposed medium effect.

Acknowledgements

Supported in part by KFA Jülich, COSY Collaboration 41126865.

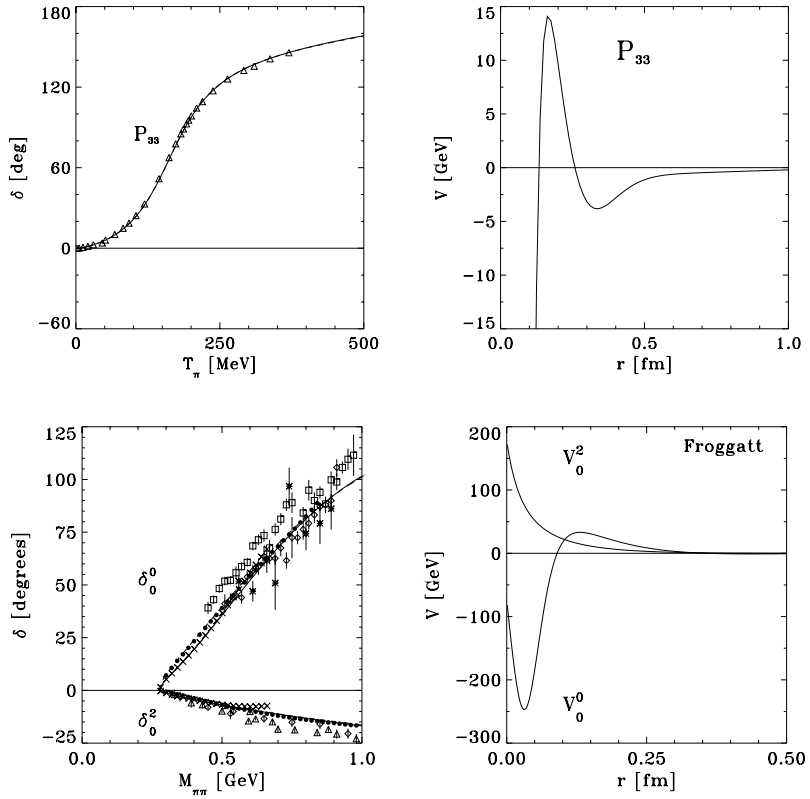

Figure 7: Quantum inversion of the πN (top) and $\pi\pi$ system (bottom) with their respective potentials.

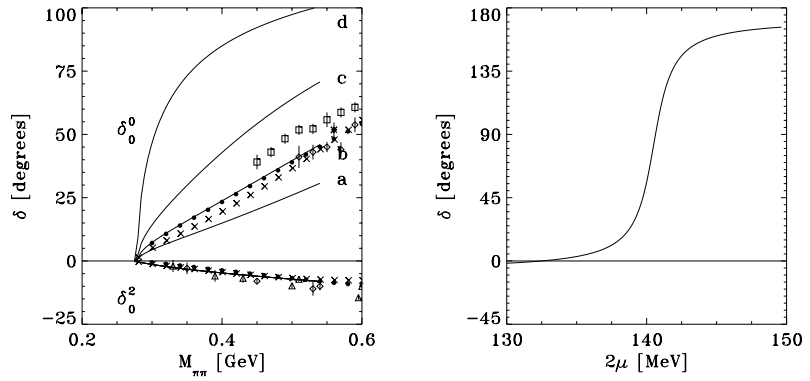

Figure 8: Study of the $\pi\pi$ s–wave scattering phase shifts with regards to small variations of the pion mass. The inversion potentials of Fig. 7 (bottom) are used. The right side shows the phase variation as a function of the pion mass for $M_{\pi\pi} = 500$ MeV.

References

[1] H. Feshbach, *Theoretical nuclear physics: nuclear reactions*, Wiley (1992)

[2] L. Ray, G.W. Hoffmann and W.R. Coker, Phys. Rep. **212**, 223 (1992)

[3] R. Rapp, J.W. Durso and J. Wambach, LANL e–print nucl–th/9611019; G. Chanfray, LANL e–print nucl–th/9607051

[4] W.G. Love and M.A. Franey, Phys. Rev. **C24**, 1071 (1981), and M.A. Franey and W.G. Love, Phys.Rev. **C31**,488 (1985)

[5] M. Lacombe, B. Loiseau, J. M. Richard, R. Vinh Mau, J. Côté, P. Pirés and R. de Tourreil, Phys.Rev. C**21**, 861 (1980).

[6] R. Machleidt, K. Holinde and Ch. Elster, Phys.Rep. **149**, 1 (1987), R. Machleidt, in *Advances in Nuclear Physics 19* , (Eds.) J.W. Negele and E. Vogt, Plenum (1989), R. Machleidt and G.Q. Li, Phys. Rep. **242**, 5 (1994)

[7] L. Jäde and H.V. von Geramb, Phys. Rev. C to appear 1/1997

[8] V.G.J. Stocks, R.A.M. Klomp, C.P.F. Terheggen and J.J. de Swart, Phys.Rev. C**49**, 2950 (1994), and cited references

[9] H.V. von Geramb and H. Kohlhoff, in *Quantum inversion theory and applications*, Lecture Notes in Physics **427**, Springer (1994), and related material Hamburg (1985–96)

[10] J.P. Jeukenne, A. Lejeune and C. Mahaux, Phys. Rep. **C25**, 83 (1976), and C. Mahaux Nucl. Phys. **A396**, 9c (1983)

[11] W. Glöckle et al, in *Few–Body Problems in Physics '95*, Few Body Systems Suppl. **8**, Springer (1996)

[12] H.F. Arellano, F.A. Brieva, M. Sander and H.V. von Geramb, Phys. Rev. **C54**, 2570 (1996)

[13] J.M.J. van Leeuwen and A.S. Reiner, Physica **27**, 99 (1961), and M.G. Fuda and J.S. Whiting, Phys. Rev. **C8**, 1255 (1973)

[14] H.V.v.Geramb and K.A.Amos, Phys. Rev. **C41** 1384 (1990), and M. Jetter, H. Freitag and H.V. von Geramb, Physica Scripta **48**, 229 (1993)

[15] H.F. Arellano, F.A. Brieva and W.G. Love, Phys. Rev. **C52**, 301 (1995).

[16] H.F. Arellano, F.A. Brieva and W.G. Love, Phys. Rev. **C41**, 2188 (1990).

[17] Ch. Elster, T. Cheon, E.F. Redish and P.C. Tandy, Phys. Rev. C**41**, 814 (1990).

[18] R. Crespo, R.C. Johnson and J.A. Tostevin, Phys. Rev. C**41**, 2257 (1990).

[19] H.F. Arellano, F.A. Brieva and W.G. Love, Phys. Rev. **C50**, 2480 (1994).

[20] H.V.v.Geramb, K.A.Amos, L.Berge, S.Bräutigam, H.Kohlhoff, A.Ingemarsson, Phys. Rev. **C44** (1991) 73

[21] J. Raynal, DWBA91, Saclay (1991)

[22] R. Schaefer and J. Raynal, DWBA70, Saclay (1970)

[23] M. Jetter, thesis, Hamburg (1993), and Phys. Rev. C49, 1832 (1994)

[24] M. Sander, thesis, Hamburg (1996); L. Jäde, M. Sander and H.V. von Geramb, LANL e–print server nucl–th/9609054; M. Sander and H.V. von Geramb, LANL e–print server nucl–th/9611001

[25] R.A. Arndt, SAID, Virginia Polytechnic Institute, and R. A. Arndt, I. I. Strakovsky and R. L. Workman, Phys. Rev. **C50**, 2731 (1994).

[26] Log into `i04ktha.desy.de` as user `anonymous`